Rev. Adv. Mater. Sci. 47 (2016) 42-48

MOLECULAR DYNAMICS SIMULATION OF THE EFFECT OF ULTRASONIC VIBRATIONS ON THE STRUCTURE OF NONEQUILIBRIUM [112] TILT GRAIN BOUNDARIES IN NICKEL

A. A. Nazarov

Institute for Metals Superplasticity Problems, Russian Academy of Sciences,
39 Khalturin str., 450001 Ufa, Russia

Received: July 14, 2016

Abstract. The effect of ultrasonic vibrations on the structure of nonequilibrium symmetric [112] tilt grain boundaries (GBs) in nickel containing dipoles of wedge disclinations is studied by means of molecular dynamics simulations. As an example, symmetrical $\Sigma = 15$ / 78.46° tilt boundary is considered. It is shown that above some critical amplitude of the applied oscillating tensile stress the GB acts as a source of lattice dislocations the generation of which relaxes the internal stresses and excess energy associated with the disclination dipole. After several cycles of vibrations the GB fully recovers its equilibrium structure free of defects and long range stresses. It is concluded that the emission of lattice dislocations is an important mechanism, which leads to a number of effects related to structure relaxation in ultrafine grained materials under ultrasonic treatment observed in experiments.

1. INTRODUCTION

Ultrasonic treatment (UST) has been known as an effective method of material treatment, which allows for a significant modification of the structure and properties of materials [1]. When applied during crystallization, UST results in a more homogeneous, fine grained microstructure of as-cast metals and alloys [2].One of the well-known effects of ultrasound is the enhancement of dislocation mobility and softening during plastic deformation referred to as the acoustoplastic effect [3]. This effect is widely used in industrial processes of metal forming such as rolling, drawing, upsetting, etc. [4,5].

High-power UST is used for surface finish treatment and strain-hardening of materials [6]. In a number of studies it has been demonstrated that such a treatment can form a significantly hardened nanostructured layer near the surfaces of materials [7-9].

At moderate amplitudes the UST can have an opposite effect resulting in a decrease of internal stresses and softening of material subjected to preliminary deformation [1]. Theoretical studies have shown that ultrasound at stress amplitudes, which are less than the stresses for dislocation generation, can lead to a self-organization of dislocations into low-energy arrays thus making the structure of materials more perfect [10,11].

Of a particular interest is the effect of UST on bulk ultrafine grained (UFG) materials processed by severe plastic deformation methods. These materials exhibit a number of extraordinary mechanical properties such as very high strength, wear resistance and fatigue limit [12,13]. At the same time, a highly nonequilibrium structure of these materials, which is characterized by distortions of the crystal lattice induced mainly by grain boundary defects, causes a relatively low thermal stability of the

Corresponding author: A.A. Nazarov; e-mail: aanazarov@imsp.ru

microstructure, lower ductility and impact toughness of UFG materials as compared to those of coarse grained materials.

Recently, we carried out a series of experiments to elucidate the possibility of stabilization of microstructure and improvement of properties of UFG nickel by means of UST [14-19]. Relaxation of non-equilibrium grain boundaries and triple junctions, reduction of internal strains and an increase of the thermal stability of nanostructured Ni processed by high pressure torsion has been discovered [14,15]. For Ni processed by equal-channel angular pressing, it was demonstrated that the UST resulted in a considerable increase of total elongation at room temperature without a loss of the strength and a significant enhancement of the impact toughness [16-19]. In [18,19] a possible mechanism of the structure relaxation in UFG metals under the effect of ultrasound has been proposed according to which a combined action of oscillating applied stress and internal stressed associated by junction disclinations results in a generation of lattice dislocations and their sink to GBs to compensate the disclinations. This model, however, cannot predict how and where these dislocations are generated.

In the present paper we examine the generation of lattice dislocations from a GB containing a disclination dipole by means of molecular dynamics. This study gives an insight into the atomistic mechanism of the relaxation of nonequilibrium GBs under ultrasonic irradiation.

2. GRAIN BOUNDARY MODEL AND SIMULATION PROCEDURE

A tilt GB with misorientation axis [112] in a f.c.c metal, nickel, will be considered. This model is chosen due to its convenience in the study of lattice dislocation - GB interactions, since deformation of the grains of this system occurs by a glide of dislocations of a single slip system. Quite recently, studies of dislocation emission from GBs of this type have been carried out for aluminum [20]. In our model, interatomic interactions in nickel were described by the embedded atom method (EAM) potential developed by Foiles, Daw and Baskes [21]. This potential is fitted to the lattice parameter a_0 = 3.52 Å, cohesive energy ε_0 = 4.45 eV and other characteristics of nickel. The computation cell is constructed as follows.

First, a bicrystal with a defect-free tilt GB with inverse coincidence site density Σ = 15 and misorientation angle θ = 78.46° is constructed. The *z*-axis of the computation cell is directed along the common crystallographic axis [112], and *y*-axis lies along the normal to tilt axis in the GB plane (Fig. 1). In these directions periodic boundary conditions are applied. Accordingly, the sizes of the computation cell along *z* and *y* axes are equal to H_z = 3/2[112] = 12.93 Å and $H_y = 20h_y$ = 157.4 Å respectively, where $h_y = a_0\sqrt{5}$ is the period of tilt GB Σ = 15 / θ = 78.46°. In the direction of *x* axis the system had a finite size equal to H_x = 150 Å and, respectively, open surfaces. Thus, the dislocations emitted from the GB were able to sink at the surfaces. This model also allows for a back emission of dislocations from the surfaces, when the sign of applied stress is changed, if the sum of applied and internal stresses is enough for their generation. In order to exclude high energy surface atoms from the calculation of total potential energy of the system, atomic layers with the thickness of 15 Å were selected near each surface.

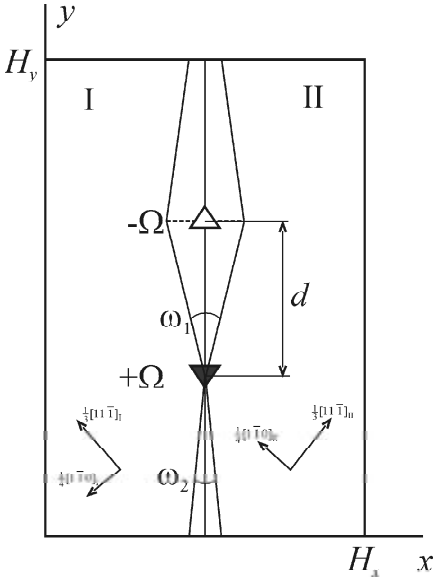

Fig. 1. A schematic description of a computation cell for the simulation of a nonequilibrium grain boundary with a disclination dipole.

As the next step of initial system construction, a dipole of wedge disclinations is introduced in the central part of the GB by making and closing a cut with two wedge angles ω_1 and ω_2 as shown in Fig. 1. These angles obey the obvious geometric relation $d\tan(\omega_1/2) = (H_y - d)\tan(\omega_2/2)$. The arm of the dipole had the value of d = 50 Å. Thus, for the chosen value of ω_1, ω_1 = 10°, we have ω_2 = 4.7°, and the strength of disclination dipole introduced is equal Ω = 14.7°. It should be pointed out that this value of disclination strength is far below the critical value above which the defect can result in the formation

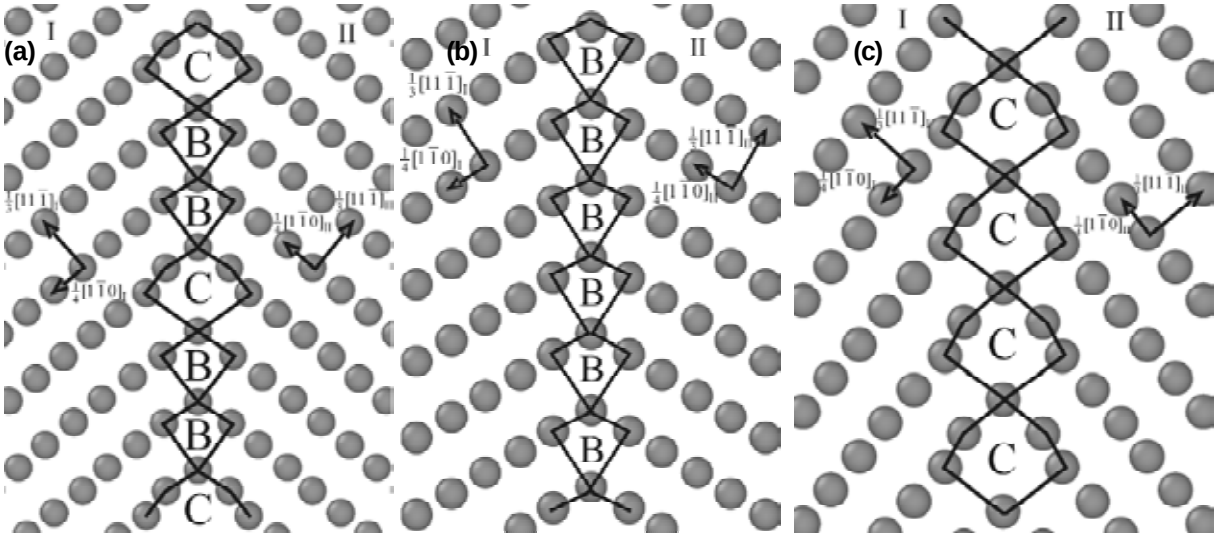

Fig. 2. Atomic structures of equilibrium [112] tilt GBs Σ = 15/78.46° (a), =11/62.96° (b), and Σ = 5/101.54° (c). The Σ = 15 is an intermediate GB, which consists of structural units of two delimiting GBs Σ = 11 (units B) and Σ = 5 (units C).

of a crack. This critical value was estimated in Ref. [22], where the following formula was derived for a disclination in a bicrystalline cylinder of nickel with radius R: $\Omega_c \approx 55.7°/\sqrt{R}$, where R is substituted in nanometers. For a disclination dipole, the screening distance of stress fields scales with its arm, therefore, d should be substituted into this formula. This yields $\Omega_c \approx 24° > \Omega$.

One should also note that, since along the y axis periodic boundary conditions are applied, in fact we simulate the effect of not a single disclination dipole, but of a disclination dipole wall with a period H_y. Although this wall has an exponentially decaying long-range stress field [23], its short-range stresses are similar to those of a single dipole. In the present case it is these short range stresses that play the most important role in dislocation emission from the GB, so the results will be valid for an isolated disclination dipole in a boundary.

The system constructed by the procedure described above consisted of 27198 atoms. This system was first relaxed at zero temperature to minimize the energy and then subjected to molecular dynamics run for 100 ps with time step 2 fs at a temperature 300 K. The simulations were carried out by molecular dynamics code XMD [24].

The bicrystal with relaxed structure was subjected to oscillating straining at the same temperature of 300K by applying a sinusoidal stress along the y axis: $p_y = p_{y0}[\sin(2\pi/\tau)t]$, the period of which was equal to τ = 160 ps. Coordinates of the particles were recorded in an *XYZ* format file with a time step 2 ps in order to visualize the dynamics of structural changes during straining. Atomic energies were saved after each loading cycle. Visualization of the structures was done using the code OVITO [25]. Simulations were carried out for four values of the stress amplitude p_{y0}= 1, 1.5, 1.7, and 2 GPa.

In order to catch average positions of vibrating atoms at 300K and calculate their potential energies more correctly, each state to analyze was finally subjected to a very short, 200 time steps energy minimization.

The results of simulations were analyzed in terms of observing the GB structure changes and lattice dislocation emission during deformation, changes of the simulation cell size H_y, and the change of the total energy of the system (except for surface layer atoms) with the number of cycles.

In order to describe the structure of reference GB Σ = 15 / 78.46° in terms of structural unit model [26] and estimate the excess energy of the GB due to the disclination dipole, structures of three equilibrium [112] tilt GBs, Σ = 15/78.46°, Σ = 11/62.96°, and Σ = 5/101.54° were also simulated and their energies were calculated.

3. SIMULATION RESULTS

Presented in Fig. 2 are the atomic structures of equilibrium tilt GBs Σ = 15/78.46°, Σ = 11/62.96°, and Σ = 5/101.54°. One can see that the structure of Σ = 15 GB is decomposed into structural units of the two delimiting GBs, Σ = 11 and Σ = 5. This is consistent with the structural unit model for tilt GBs in general [26] and that for [112] tilt GBs in particular

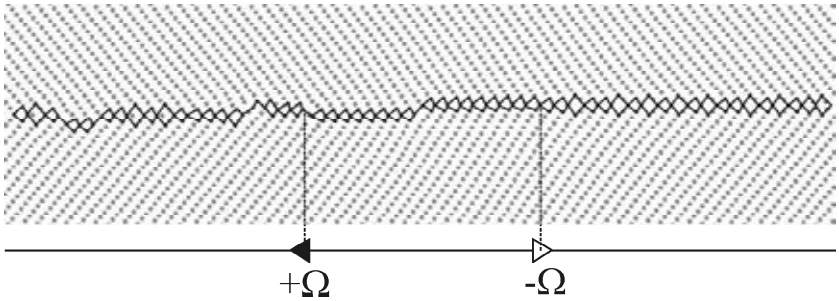

Fig. 3. Relaxed structure of Σ = 15 tilt GB with a disclination dipole at 300K.

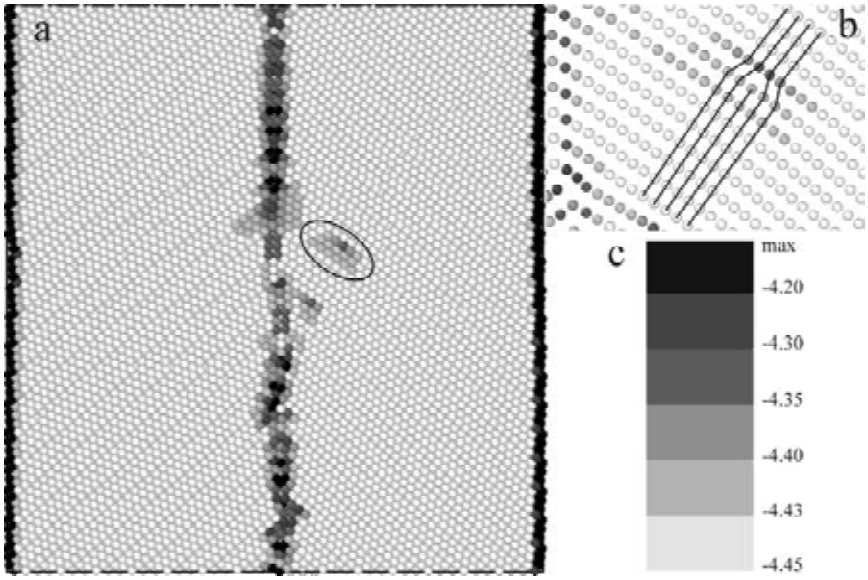

Fig. 4. Atomic energy map of nonequilibrium Σ = 15 GB with a disclination dipole after relaxation at 300K (a), a magnified image of lattice dislocation located near the GB in the region indicated by an ellipse (b) and energy levels (c).

[20]. Energies of the three GB calculated after zero-temperature relaxation are equal to $\gamma = 1.25$ Jm^{-2} for Σ = 15, 0.54 Jm^{-2} for Σ = 11, and 1.37 Jm^{-2} for Σ = 5.

Atomic structure of the Σ = 15 GB containing a disclination dipole relaxed at 300K is represented in Fig. 3. For a convenience, the coordinate frame and the picture are turned to 90° clockwise with respect to Fig. 1. One can see that outside the region between disclinations, the GB structure is still described by a sequence of B and C type structural units, albeit several steps on the GB plane are formed. Between the disclinations, due to a change of the misorientation angle, the GB structure is very close to that of Σ = 11 GB. Steps are observed in this region too.

Fig. 4 represents a map of atomic energies in this system. One can see GB atoms have mostly high energies. Comparing the intensities of the black color in the GB and lattice dislocation core in the region indicated by an ellipse, one can see that atomic energies in the GB are significantly higher than in the dislocation core.

The energy map after three cycles of deformation by an application of periodic stress $p_y = p_{y0}[\sin(2\pi/\tau)t]$ with amplitude $p_{y0} = 1.7$ GPa is presented in Fig. 5. A comparison of Figs. 3 and 5 obviously shows that a significant reduction of atomic energies in the GB region occurred. Also one can see a change of the shape of the bicrystal, decrease of its size in the *y* direction. A close examination of snapshots taken with 2 ps time intervals shows that this is a consequence of plastic deformation carried out by lattice dislocations, which are emitted from the GB, glide over the grains and exit to the surfaces of the bicrystal. One of such dislocations is depicted in Fig. 6. The dislocations are emitted only from the GB regions above the negative disclination (see Fig. 1), i.e. at $y>(H_y + d)/2$, and below the positive disclination, i.e. at $y<(H_y - d)/2$. As a result of this process, the misorientation angle of corresponding parts of the GB decreases and approaches that of Σ = 11 / 62.96° GB. Eventually, the initially nonequilibrium GB relaxes all over its length to a nearly perfect Σ = 11 tilt GB with a low energy.

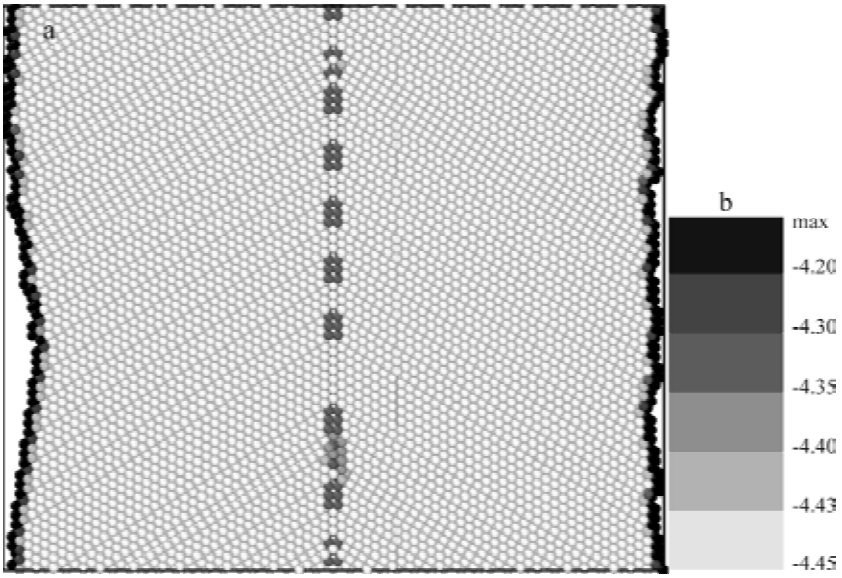

Fig. 5. Atomic energy map of Σ = 15 GB with a disclination dipole after three cycles of deformation by periodic stress with amplitude 1.7 GPa (a) and energy levels (b).

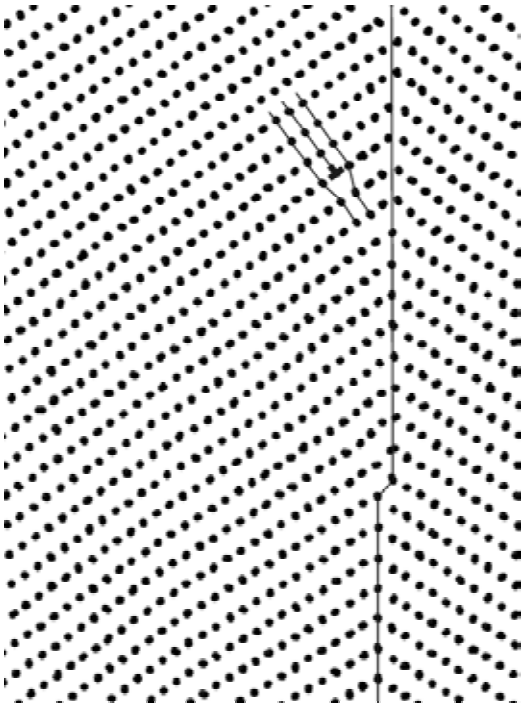

Fig. 6. Lattice dislocation emitted from the GB during periodic deformation. The position of GB plane is shown by a vertical line.

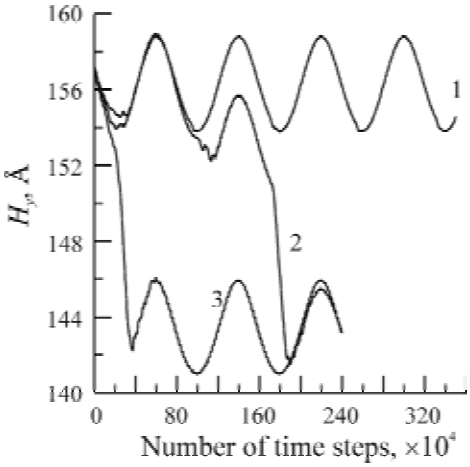

Fig. 7. Change of simulation size H_y with the number of time steps during oscillating loading with different amplitudes: p_y = 1.5 (a), 1.7 (b), 2.0 (c) GPa.

As the simulations show, the process of dislocation emission is asymmetric with respect to the applied stress. Dislocations are emitted from the GB, when the applied shear stress is added to the internal stress from disclinations, go across the grains and sink at surfaces during the same half-period. When the sign of applied stress is changed, the surfaces cannot emit the dislocations back, probably due to the fact that this requires a higher local stress. Moreover, the internal stress of the GB is now has the sign opposite to that of the applied one.

Presented in Fig. 7 are the dependencies of the simulation cell size H_y on MD time step numbers for three different amplitudes of oscillating stress. One can see that nearly no plastic deformation and therefore no dislocation emission occurs at p_y = 1.5 GPa up to five cycles. At p_y = 1.7 GPa dislocation emission begins during the second cycle and completes during the third cycle. At p_y = 2.0 GPa all dislocations are emitted and the GB relaxation is completed during the first cycle. This result is confirmed also by Fig. 8 where the changes of

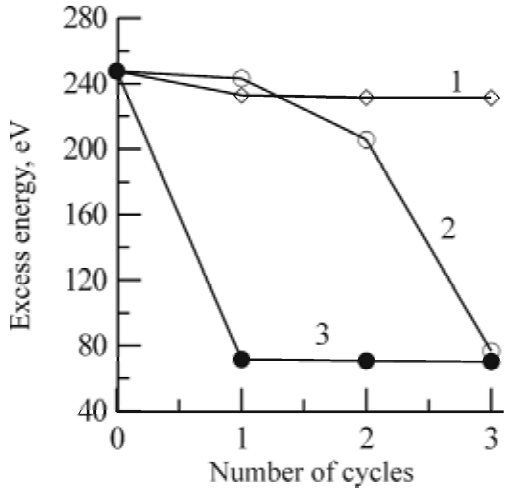

Fig. 8. Change of the excess energy of simulation cell (except for surface layer atoms) with the number of oscillating loading cycles with different amplitudes: p_y= 1.5 (a), 1.7 (b), 2.0 (c) GPa.

simulation cell excess energy on the number of cycles are presented. For the first stress amplitude only a slight relaxation of energy occurs, while at higher amplitudes a complete energy relaxation is reached. A calculation shows that the energies level off at the value corresponding to the energy of equilibrium Σ = 11 tilt GB.

4. DISCUSSION

The present simulations show that an application of an oscillating stress on a bycrystalline material the GB of which contains a disclination-type defect can result in the relaxation of its nonequilibrium structure. Applied stress, when it is added to the internal stresses induced by defects, leads to an emission of lattice dislocations, which compensate the GB defects. This process is asymmetric, since the dislocations sink at the surfaces and are not emitted back during the change of applied stress sign. This can be extrapolated for the case of a polycrystalline material, where normally lattice dislocations are confined to grains and cannot always sink at surfaces. Instead, they will be absorbed by opposite GBs or react with dislocations emitted from the latter. Since junction disclinations in deformed polycrystals form quadupole or even higher-order multipoles [12,27], this process in general tends to reduce the internal stresses of defects and will be asymmetric too. Thus, the conclusion on the relaxation of nonequilibrium GB structure under ultrasonic treatment will be valid for real polycrystals too.

The result obtained in the present work is similar to that reported recently by Rupert and Schuh [28]. These authors studied the effect of cyclic loading-unloading on the structure and strength of a model nanocrystalline nickel constructed by a Voronoi tessellation. It is suggested that the as-constructed nanocrystal is in a nonequilibrium state. A reconstruction of its structure, relaxation of GBs, reduction of their energy and an increase of the yield stress of the nanocrystal during post-treatment simulated tension tests were observed after cycling. The character of nonequilibrium GB structure in the cited study is, however, significantly different from that studied in the present paper. The model nanocrystal constructed by Voronoi tessellation is similar to a real nanocrystal prepared by crystallization from liquid or amorphous states. These materials can have metastable structural states with a range of energies like amorphous alloys and the relaxation of these states normally requires only short-range atomic rearrangements. On contrary, the noneqiulibrium state of GBs simulated here is typical for UFG or nanostructured materials prepared severe plastic deformation and is caused by extrinsic grain boundary dislocations absorbed during plastic deformation [12]. The relaxation of this state requires either a long-range diffusion of atoms to the distances of the order of grain size at high temperature annealing [29] or generation of dislocations during mechanical cycling as it has been observed in the present case.

During our simulations dislocation emission was observed only at very high applied stresses and at the very beginning of stress oscillations. This is common for such idealized systems and for short time intervals available for molecular dynamics simulations. In real cases, the process would occur even at much lower stresses due to some thermal activation, while the incubation time for each dislocation emission event would be much longer. Thus, one can expect that relaxation of nonequilibeium GBs in real UFG metals occurs at reasonable amplitudes of ultrasound and during reasonable time intervals.

5. CONCLUSION

Thus, on an example of a bicrystal whose GB contains a disclination dipole we have demonstrated that the application of a periodic tension-compression stress to a deformed material results in a relaxation of the nonequlibrium structure of grain boundaries. The microscopic mechanism for this relaxation is the emission of lattice dislocations by grain boundaries by which way they compensate their defect structures. As a result of emission of

dislocations and their glide to appropriate sinks and overall relaxation of deformed polycrystal into its equilibrium, defect free structure can occur. This can be suggested as an underlying mechanism of the effect of ultrasonic treatment on the structure and properties of UFG materials processed by deformation methods.

ACKNOWLEDGEMENT

This work was supported by the Russian Science Foundation under the grant No. 16-19-10126.

REFERENCES

[1] A.V. Kulemin, *Ultrasound and Diffusion* (Metallugia Publ., Moscow, 1978), In Russian.
[2] O.V. Abramov, *Ultrasound in Liquid and Solid Metals* (CRC Press, Boca Raton, 1994).
[3] F. Blaha and B. Langenecker // *Naturwissenschaften* **42** (1955) 556.
[4] V.P. Severdenko, V.V. Klubivich and A.V. Stepanenko, *Metal Forming with Ultrasound* (Nauka I Tekhnika, Minsk, 1973), In Russian.
[5] O.V. Abramov, I.G. Khorbenko and Sh. Shvegla, *Ultrasonic Treatment of Materials* (Mashinostroenie, Moscow, 1984), In Russian.
[6] V.V. Klubovich, V.V. Artemyev and V.N. Sakevich, *Ultrasonic Vibroimpulsive Processes* (Belarus Nat. Tech. Univ., Minsk, 2004), In Russian.
[7] A.V. Panin, E.A. Melnikova, O.B. Perevalova, Yu.I. Pochivalov, M.V. Leontyeva-Smirnova, V.M. Chernov and Yu.F. Ivanov // *Physical Mesomechanics* **12** (2009) 150.
[8] Yu.R. Kolobov, O.A. Kashin, E.F. Dudarev, G.P. Grabovetskaya, G.P. Pochivalova, V.A. Klimenov, N.V. Girsova and E.E. Sagymbaev // *Russian Physics Journal* **43 (**2000) 754.
[9] A.I. Lotkov, A.A. Baturin, V.N. Grishkov, Zh.G. Kovalevskaya and P.V. Kuznetsov // *Technical Physics Letters* **31** (2005) 912.
[10] A.A. Nazarov and Sh.Kh. Khannanov // *Fizika I Khimia Obrabotki Materialov* **4** (1986) 109, In Russian.
[11] N.A. Tyapunina, E.K. Naimi and G.M. Zinenkova, *Effect of Ultrasound on Crystals with Defects* (Moscow State Univ., Moscow, 1999), In Russian.
[12] A.A. Nazarov and R.R. Mulyukov, In: *Handbook of Nanoscience, Engineering, and Technology*, ed. by W. Goddard, D. Brenner, S. Lyshevski and G. Iafrate (Boca Raton: CRC Press, 2002), p.22-1.
[13] R.Z. Valiev, A.P. Zhilyaev and T.G. Langdon, *Bulk Nanostructured Materials: Fundamentals and Applications* (Wiley, Hoboken, 2013).
[14] A.A. Nazarova, R.R. Mulyukov, V.V. Rubanik, Yu.V. Tsarenko and A.A. Nazarov // *Phys. Metals Metallogr.* **110** (2010) 574.
[15] A.A. Nazarova, R.R. Mulyukov, Yu.V. Tsarenko, V.V. Rubanik and A.A. Nazarov // *Mater. Sci. Forum*. **667-669** (2011) 605.
[16] A.A. Samigullina, R.R. Mulyukov, A.A. Nazarov, A.A. Mukhametgalina, Yu.V. Tsarenko and V.V. Rubanik // *Letters on Materials* **4** (2014) 52.
[17] A.A. Samigullina, Yu.V. Tsarenko, V.V. Rubanik, V.A. Popov, V.N. Danilenko and R.R. Mulyukov // *Letters on Materials* **2** (2012) 214.
[18] A.A. Nazarov, A.A. Samigullina, R.R. Mulyukov, Yu.V. Tsarenko and V.V. Rubanik // *Journal of Machinery Manufacture and Reliability* **43** (2014) 153-159.
[19] A.A. Samigullina, A.A. Nazarov, R.R. Mulyukov, Yu.V. Tsarenko and V.V. Rubanik // *Rev. Adv. Mater. Sci*. **39** (2014) 14.
[20] T. Shimokawa // *Phys. Rev. B* **82** (2010) 174122.
[21] S.M. Foiles, M.I. Daw and M.S. Baskes // *Phys. Rev. B* **33** (1986) 7983.
[22] K. Zhou, M.S. Wu and A.A. Nazarov // *Phys. Rev. B* **73** (2006) 045410.
[23] V.Yu. Gertsman, A.A. Nazarov, A.E. Romanov, R.Z Valiev and V.I. Vladimorov // *Philos. Mag. A* **59** (1989) 1113.
[24] http://xmd.sourceforge.net/about.html.
[25] A. Stukowski // *Modell. Simul. Mater. Sci. Eng.* **18** (2010) 015012.
[26] A. P. Sutton and R. W. Balluffi, I*nterfaces in Crystalline Materials* (Oxford, Oxford Science Publishers, 1995).
[27] A.A. Nazarov // *Scripta Mater*. **37** (1997) 1155.
[28] T.J. Rupert and C.A. Schuh // *Phil. Mag. Lett.* **92** (2012) 20.
[29] A.A. Nazarov // *Interface Sci.* **8** (2000) 315.